



Addendum: A dispersive analysis of $\eta' \rightarrow \pi^+\pi^-\gamma$ and $\eta' \rightarrow \ell^+\ell^-\gamma$

Simon Holz^{1,a}, Christoph Hanhart², Martin Hoferichter¹, Bastian Kubis³

¹ Albert Einstein Center for Fundamental Physics, Institute for Theoretical Physics, University of Bern, Sidlerstrasse 5, 3012 Bern, Switzerland
² Forschungszentrum Jülich, Institute for Advanced Simulation, Institut für Kernphysik, and Jülich Center for Hadron Physics, 52425 Jülich, Germany
³ Helmholtz-Institut für Strahlen- und Kernphysik and Bethe Center for Theoretical Physics, Universität Bonn, 53115 Bonn, Germany

Received: 22 November 2022 / Accepted: 30 November 2022
 © The Author(s) 2022

Abstract In this addendum to Ref. [1] we show that the mismatch between the ρ - ω mixing parameter $\epsilon_{\rho\omega}$ as extracted from $\eta' \rightarrow \pi^+\pi^-\gamma$ and $e^+e^- \rightarrow \pi^+\pi^-$ can be resolved by including higher orders in the expansion in e^2 in the description of the $\eta' \rightarrow \pi^+\pi^-\gamma$ decay. We repeat the analysis in this extended framework and update the numerical results accordingly.

Addendum to: Eur. Phys. J. C

<https://doi.org/10.1140/epjc/s10052-022-10247-7>

1 Extended formalism

Following the notation from Ref. [1] throughout, the spectrum for $P \rightarrow \pi^+\pi^-\gamma$ can be expressed as

$$\frac{d\Gamma(P \rightarrow \pi^+\pi^-\gamma)}{ds} = 16\pi\alpha\Gamma_0|F_\pi^V(s)|^2 \left| P(s)(1 + \Pi_\pi(s)) - \frac{e^2 F_{P\gamma\gamma}}{s} - \frac{g_{P\omega\gamma}}{g_{\omega\gamma}} \frac{\epsilon_{\rho\omega} - e^2 g_{\omega\gamma}^2}{M_\omega^2 - s - iM_\omega\Gamma_\omega} \right|^2, \quad (1.1)$$

generalizing Eq. (D.14) in Ref. [1] by the next order in the expansion in e^2 (the sign convention is such that $g_{P\omega\gamma} < 0$). The most important change, numerically, concerns $\epsilon_{\rho\omega} \rightarrow \epsilon_{\rho\omega} - e^2 g_{\omega\gamma}^2$ in the numerator of the ω propagator, corresponding to the photon contribution in $\epsilon_{\rho\omega}$ as defined in resonance chiral perturbation theory [2–4]. In our formalism, $\epsilon_{\rho\omega}$, determined from a fit to the bare cross section for $e^+e^- \rightarrow \pi^+\pi^-$, does not include this VP effect, in line with the definition in Ref. [5] (numerically, it evaluates to $e^2 g_{\omega\gamma}^2 = 0.34(1) \times 10^{-3}$). This shift removes the tension

observed between $\eta' \rightarrow \pi^+\pi^-\gamma$ and $e^+e^- \rightarrow \pi^+\pi^-$ in Ref. [1].

The coefficients appearing in Eq. (3.9) of Ref. [1] are generalized according to Eq. (1.1):

$$\begin{aligned} \mathcal{A}_2 &= -\Gamma(\eta' \rightarrow \pi^+\pi^-\gamma) + 16\pi\alpha \int_{4M_\pi^2}^{M_{\eta'}^2} ds \Gamma_0 |F_\pi^V(s)|^2 \\ &\quad \times \left| \frac{g_{\eta'\omega\gamma}}{g_{\omega\gamma}} \frac{\epsilon_{\rho\omega} - e^2 g_{\omega\gamma}^2}{M_\omega^2 - s - iM_\omega\Gamma_\omega} + \frac{e^2 F_{\eta'\gamma\gamma}}{s} \right|^2, \\ \mathcal{A}_1 &= 32\pi\alpha \int_{4M_\pi^2}^{M_{\eta'}^2} ds \Gamma_0 |F_\pi^V(s)|^2 \operatorname{Re} \left[P_{\text{ev}}(s)(1 + \Pi_\pi^*(s)) \right. \\ &\quad \left. \times \left(\frac{g_{\eta'\omega\gamma}}{g_{\omega\gamma}} \frac{e^2 g_{\omega\gamma}^2 - \epsilon_{\rho\omega}}{M_\omega^2 - s - iM_\omega\Gamma_\omega} - \frac{e^2 F_{\eta'\gamma\gamma}}{s} \right) \right], \\ \mathcal{A}_0 &= 16\pi\alpha \int_{4M_\pi^2}^{M_{\eta'}^2} ds \Gamma_0 |F_\pi^V(s)|^2 P_{\text{ev}}^2(s) |1 + \Pi_\pi(s)|^2. \end{aligned} \quad (1.2)$$

In the following, we provide the updated numerical results when including the additional e^2 effects as given in Eq. (1.1), implemented in the fit via Eq. (1.2).

2 Numerical results

The updated fit parameters are collected in Table 1, Fig. 1, and Table 2. The main difference to the results presented in Ref. [1] is that the shift $\epsilon_{\rho\omega} \rightarrow \epsilon_{\rho\omega} - e^2 g_{\omega\gamma}^2$ removes the tension between $e^+e^- \rightarrow \pi^+\pi^-$ and the $\eta' \rightarrow \pi^+\pi^-\gamma$ spectrum, markedly improving the quality of the combined fit.

^a e-mail: holz@itp.unibe.ch (corresponding author)

Table 1 Comparison of the fit outcome of the differential decay width in Eq. (1.1) to the BESIII $\eta' \rightarrow \pi^+\pi^-\gamma$ spectrum [6] of the binned maximum likelihood and minimum χ^2 strategies. The χ^2/dof is 1.30 and 1.31, respectively, with the one of the Likelihood method extracted by means of the approximation described in App. C of Ref. [7]

Quantity	Likelihood	χ^2
A [GeV^{-3}]	17.12(35)	17.09(32)
β [GeV^{-2}]	0.714(55)	0.723(45)
γ [GeV^{-4}]	-0.412(55)	-0.420(45)
$\epsilon_{\rho\omega} \times 10^3$	1.998(67)	1.997(54)
M_ω [MeV]	782.99(33)	783.00(27)

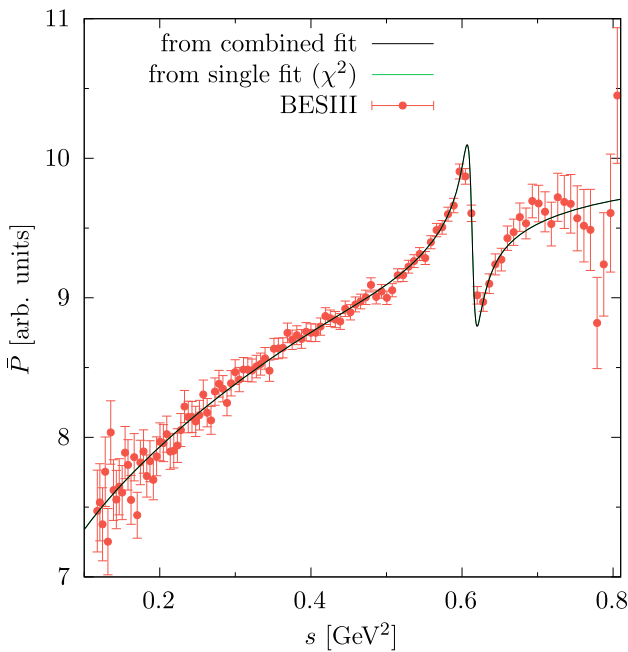


Fig. 1 Fit to the differential decay rate of $\eta' \rightarrow \pi^+\pi^-\gamma$ (individually or combined with the VFF). To highlight potential differences in the ρ - ω region, we show the associated function \bar{P} , as defined in Eq. (3.11) of Ref. [1], compared to the experimental data from BESIII [6]. The two fits cannot be distinguished on this scale

Table 2 Combined fit to several pion VFF data sets (BaBar, KLOE, CMD-2, SND) and $\eta' \rightarrow \pi^+\pi^-\gamma$ spectrum (BESIII) with overall $\chi^2/\text{dof} = 1.46$. In the row for KLOE, the three values for M_ω refer to

	χ^2/dof	M_ω [MeV]	A [GeV^{-3}]	β [GeV^{-2}]	γ [GeV^{-4}]	$\alpha_\pi \times 10^2$ [GeV^{-2}]	$\epsilon_{\rho\omega} \times 10^3$
BaBar	1.26	781.875(82)	17.10(32)	0.720(46)	-0.418(46)	5.74(14)	2.007(10)
KLOE	1.61	781.65(12)					
		782.10(17)					
		781.84(27)					
CMD-2	2.18	782.131(68)					
SND	2.16	781.457(97)					
BESIII	1.31	783.00(28)					

The updated results for the TFF are shown in Fig. 2 and Table 3. In particular, the prediction for the slope parameter

$$b_{\eta'} = 1.431(23) \text{ GeV}^{-2} \tag{2.1}$$

is reduced by about 1σ , which traces back not to the change in $\epsilon_{\rho\omega}$ (which is marginal given the fact that the fit is dominated by $e^+e^- \rightarrow \pi^+\pi^-$), but to a stronger curvature in the polynomial $P(s)$ (the coefficient γ of the quadratic term increases by a factor 3).

Acknowledgements We thank Pablo Sánchez-Puertas for pointing out the issue of one-photon-reducible contributions to $\epsilon_{\rho\omega}$, which ultimately explains the tension observed in Ref. [1]. Financial support by the SNSF (Project Nos. 200020_200553 and PCEFP2_181117), the DFG through the funds provided to the Sino-German Collaborative Research Center TRR110 ‘‘Symmetries and the Emergence of Structure in QCD’’ (DFG Project-ID 196253076 – TRR 110), and the European Union’s Horizon 2020 research and innovation programme under grant agreement No. 824093 is gratefully acknowledged.

Open Access This article is licensed under a Creative Commons Attribution 4.0 International License, which permits use, sharing, adaptation, distribution and reproduction in any medium or format, as long as you give appropriate credit to the original author(s) and the source, provide a link to the Creative Commons licence, and indicate if changes were made. The images or other third party material in this article are included in the article’s Creative Commons licence, unless indicated otherwise in a credit line to the material. If material is not included in the article’s Creative Commons licence and your intended use is not permitted by statutory regulation or exceeds the permitted use, you will need to obtain permission directly from the copyright holder. To view a copy of this licence, visit <http://creativecommons.org/licenses/by/4.0/>. Funded by SCOAP³. SCOAP³ supports the goals of the International Year of Basic Sciences for Sustainable Development.

the combinations of the global KLOE ω mass and the corresponding mass shifts of the three underlying data sets from 2008, 2010, 2012, respectively

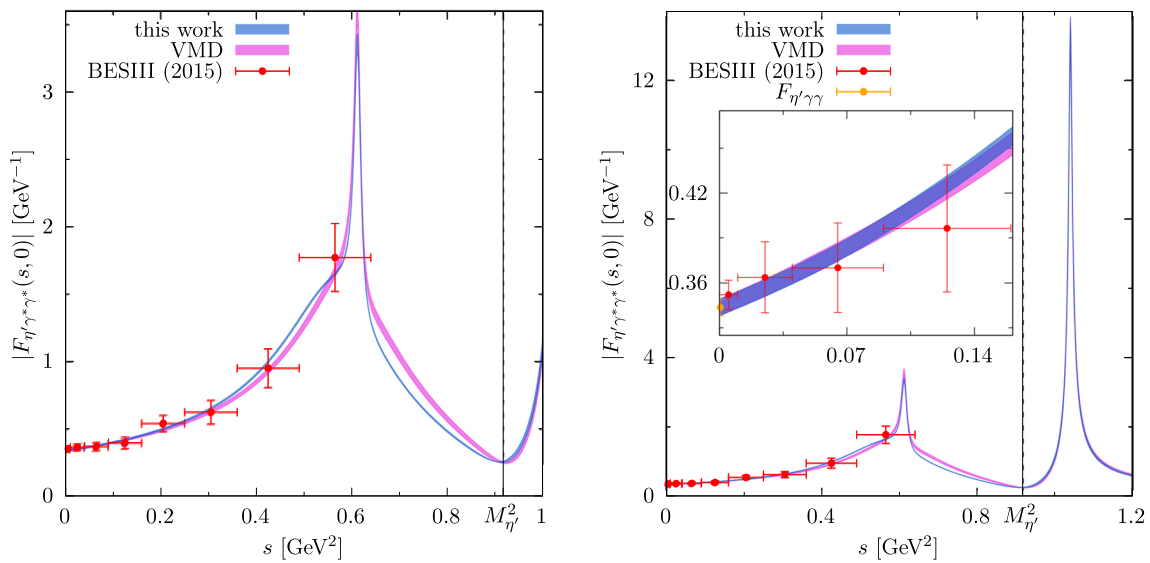


Fig. 2 Determination of the η' TFF in comparison to data from BESIII [8] (statistical and systematic errors added in quadrature) scaled with $F_{\eta'\gamma\gamma}$ and the VMD model from Ref. [1] for the ϕ resonance; for

the kinematic range accessible in η' decays (left) and a larger time-like region including the ϕ resonance with inset magnifying the low- s region (right)

Table 3 Contributions from the various components of the TFF to the sum rules of the normalization and the slope parameter

	$(I = 1)_{\epsilon_{\rho\omega}=0}$	$\Delta(I = 1)_{\epsilon_{\rho\omega}\neq 0}$	$(I = 0)_{\epsilon_{\rho\omega}=0}^\omega$	$\Delta(I = 0)_{\epsilon_{\rho\omega}\neq 0}^\omega$	$(I = 0)^\phi$	Total
Norm [%]	69.18(86)	-0.1388(19)	7.06(22)	-0.1397(47)	15.85(61)	91.9(1.1)
$b_{\eta'}$ [GeV ⁻²]	1.160(23)	0	0.1176(32)	0	0.1526(53)	1.431(23)

References

1. S. Holz, C. Hanhart, M. Hoferichter, B. Kubis, Eur. Phys. J. C **82**, 434 (2022). [arXiv:2202.05846](https://arxiv.org/abs/2202.05846) [hep-ph]
2. R. Urech, Phys. Lett. B **355**, 308 (1995). [arXiv:hep-ph/9504238](https://arxiv.org/abs/hep-ph/9504238)
3. J. Bijnens, P. Gosdzinsky, Phys. Lett. B **388**, 203 (1996). [arXiv:hep-ph/9607462](https://arxiv.org/abs/hep-ph/9607462)
4. J. Bijnens, P. Gosdzinsky, P. Talavera, Nucl. Phys. B **501**, 495 (1997). [arXiv:hep-ph/9704212](https://arxiv.org/abs/hep-ph/9704212)
5. G. Colangelo, M. Hoferichter, B. Kubis, P. Stoffer, JHEP **10**, 032 (2022). [arXiv:2208.08993](https://arxiv.org/abs/2208.08993) [hep-ph]
6. M. Ablikim et al. [BESIII Collaboration], Phys. Rev. Lett. **120**, 242003 (2018). [arXiv:1712.01525](https://arxiv.org/abs/1712.01525) [hep-ex]
7. S. Holz, Rheinische Friedrich-Wilhelms-Universität Bonn, PhD thesis (2022). <https://hdl.handle.net/20.500.11811/10336>
8. M. Ablikim et al. [BESIII Collaboration], Phys. Rev. D **92**, 012001 (2015). [arXiv:1504.06016](https://arxiv.org/abs/1504.06016) [hep-ex]